Microstructure, tensile properties of SLMed TNT5Zr-0.2O alloys without/with keyholes produced by different Post-processing treatments

Kong, Weihuan; Shi, Qi; Cox, Sophie C.; Kuang, Min; Attallah, Moataz M.

DOI:
10.1016/j.matlet.2021.131448

Document Version
Peer reviewed version

Citation for published version (Harvard):
Kong, W, Shi, Q, Cox, SC, Kuang, M & Attallah, MM 2022, 'Microstructure, tensile properties of SLMed TNT5Zr-0.2O alloys without/with keyholes produced by different Post-processing treatments', *Materials Letters*, vol. 309, 131448. https://doi.org/10.1016/j.matlet.2021.131448

Microstructure, Tensile Properties of SLMed TNT5Zr-0.2O Alloys without/with Keyholes Produced by Different Post-processing Treatments

Weihuan Kong [1], Qi Shi [2], Sophie C. Cox [3], Min Kuang [2], Moataz M. Attallah [1]*

1. School of Materials and Metallurgy, University of Birmingham, Edgbaston, B15 2TT, UK

2. Guangdong Institute of New Materials, Guangdong Academy of Science, Guangzhou, 510651, PR China

3. School of Chemical Engineering, University of Birmingham, Edgbaston, B15 2TT, UK

*Correspondence:

Moataz M. Attallah: m.m.attallah@bham.ac.uk

Abstract

Ti-34Nb-13Ta-5Zr-0.2O alloy (hereafter termed TNT5Zr-0.2O) with keyhole defects was fabricated by SLM. The microstructure and tensile properties have been investigated after two post-processing treatments, namely vacuum heat treatment (HT) and hot isostatic pressing (HIP). Microstructure shows both alloys retain beta grain matrix along with discrete nano-sized grain boundary alpha precipitates. The stress concentrations at the edge of keyholes make the voids wall collapse under tension and cracks propagate more easily in that region. Notably, the pore enclosure by HIP is not contribute to a better ductility of this alloy. This explains why the TNT5Zr-0.2O-HT alloy possesses lower UTS (978 ± 19 MPa) and elastic modulus (49 ± 3 GPa), but higher elongation (4.5% ± 0.6%) in comparison with TNT5Zr-0.2O-HIP sample.

Keywords:

Selective laser melting, Keyhole, Beta Ti alloy, Microstructure, Tensile properties

1. Introduction

Ti-Nb-Ta-Zr (TNTZ) alloys have been received intense interest for load-bearing implant development due to their ultralow Young's modulus, excellent biocompatibility and corrosion resistance [1–4]. These advantages potentially make TNTZ alloys more competent for long-term clinical use than other commercial metallic biomaterials, e.g. cobalt-based alloys, stainless steels, Ti-6Al-4V alloy. Considering these factors e.g. design flexibility, life-

cycle energy consumption of the manufactured parts, SLM technique could be a good option for manufacturing high-end biomedical components when compare with conventional manufacturing techniques [5].

One concern, mechanical stability of SLMed TNTZ alloys has been raised because the as-fabricated component involve process-induced keyhole porosity. The keyhole porosity can be typically found in high energy input SLM manufacturing. As rear part of molten pool bears with intensive local evaporation due to incident beam reaction, then dynamic recoil pressure of vapor jet and surface tension pressure dent the adjacent wall, thus it forms keyhole [7,8]. Hot isostatic pressing (HIP) that involves simultaneous function of elevated temperature and high pressure applied with inert gas in a specific vessel, has been reported to remove this defect in SLMed Ti-6Al-4V alloy [9]. In this process, argon atoms are pressed every surface of a component in a normal direction like "hot forge", thus pores are eliminated from the component after long-time dwell with proper reaction [10]. As HIP treatment of TNTZ alloys is normally arranged at high temperature, it inevitably forms cooling rate dependent microstructure. According to the former thermo-mechanical treatment results, Banerjee et al. [11], Nag et al. [12] both observed relatively large beta grains with grain boundary α precipitates in Ti-34Nb-9Zr-8Ta alloy, which was homogenized at 1100℃ for 7 days then furnace cooled. In this study, we investigate the interplay between microstructure, porosity and tensile properties of SLMed TNT5Zr-0.2O alloys without/with keyholes manufacturing by HIP and vacuum heat treatment (HT).

2. Material and methods

Spherical Ti, Zr powder (TLS) with nominal particle size distribution (15—83 μm) and (10—45 μm), rocky Nb (Elite), Ta powder (H.C. Starck) with an average particle size (D50) of 43.9 μm and 23.4 μm were blended in a horizontal rotating drum to prepare Ti-34Nb-13Ta-5Zr alloy (wt. %) feedstock. Ti-34Nb-13Ta-5Zr-0.2O alloy (hereafter termed TNT5Zr-0.2O) was obtained when perform *in-situ* alloying TNT5Zr due to the deteriorated seal in SLM system. The oxygen level in the SLMed alloy was measured using inert gas fusion standard testing [13]. The optimized SLM parameter for manufacturing cubes and tensile specimens were: 300 W laser power, 500 mm/s scanning speed, 50 μm scanning spacing, 5 x 5 mm chessboard scan strategy, and 20 μm layer thickness. Advanced HIP (Quintus, Sweden) was used to tune the microstructure of TNT5Zr-0.2O alloy. The investigated process parameters were: 3 hours dwell at 1000℃ in a container filled with 120 MPa pressurized argon atmosphere, followed by intermediate cooling rate (100℃/min). Vacuum furnace (TPF 60,

TAV Engineering) with the same parameter (1000℃×3 hours×100℃/min) was used to mainly compare the tensile properties difference between TNT5Zr-0.2O alloy with and without keyhole porosity.

OM images of as-HIPed and as-HTed TNT5Zr-0.2O alloy were captured by microscope (Axioskop 2, Zeiss) and the overlapping tiled images over a defined area were acquired through AxioVision software. The phase identification was performed by XRD (AXRD, Proto) with Cu Kα radiation, and XRD spectra were collected by a fixed parameter of 0.02ºstep size and a 2s time/step. Thin foils for TEM were prepared through argon ion milling technique (Gatan PIPS, Ametek). In order to reveal the microstructure of as-HIPed TNT5Zr-0.2O alloy, TEM (Talos F200X, FEI) was used to capture HAADF images along grain boundary. Specimens (SLM-processed original side surface) in tensile testing were carried out perpendicularly to the build direction at room temperature. The stress-strain curves were measured at a crosshead speed of 0.5 mm/min at room temperature using a tensile testing machine (2500, Zwick/Roell), and a clip-on extensometer was attached to 15 mm gage length of specimen for strain measurement until rupture. Then tensile fracture morphology was observed using ESEM (XL-30, Philips).

3. Results and discussions

Fig. 1a and Fig. 1b show OM images without etching of the as-HIPed and as-HTed TNT5Zr-0.2O alloy. Obviously, the randomly distributed keyhole porosity formed in SLM process is removed by HIP, and still maintains in vacuum HT. As TNT5Zr alloy possesses narrow temperature gap (270℃) between the lowest boiling point element Ti and highest melting point Ta, therefore the keyhole formation risk is high because local element evaporation occurs when laser beam scanning. Fig. 1c reveals the microstructure of as-HIPed TNT5Zr-0.2O alloy with discrete nano-sized grain boundary alpha precipitates. The magnitude of solute redistribution of Ti atoms from the matrix towards grain boundaries is moderately high at the HIP temperature, and the intergranular precipitates possess time for growth when undergo intermediate cooling. The presence of α phase peak along with the primary beta phase peaks is revealed in both as-HIPed and as-HTed TNT5Zr-0.2O alloys (Fig. 1d), which

confirms both alloys retain the same microstructure without/with keyholes.

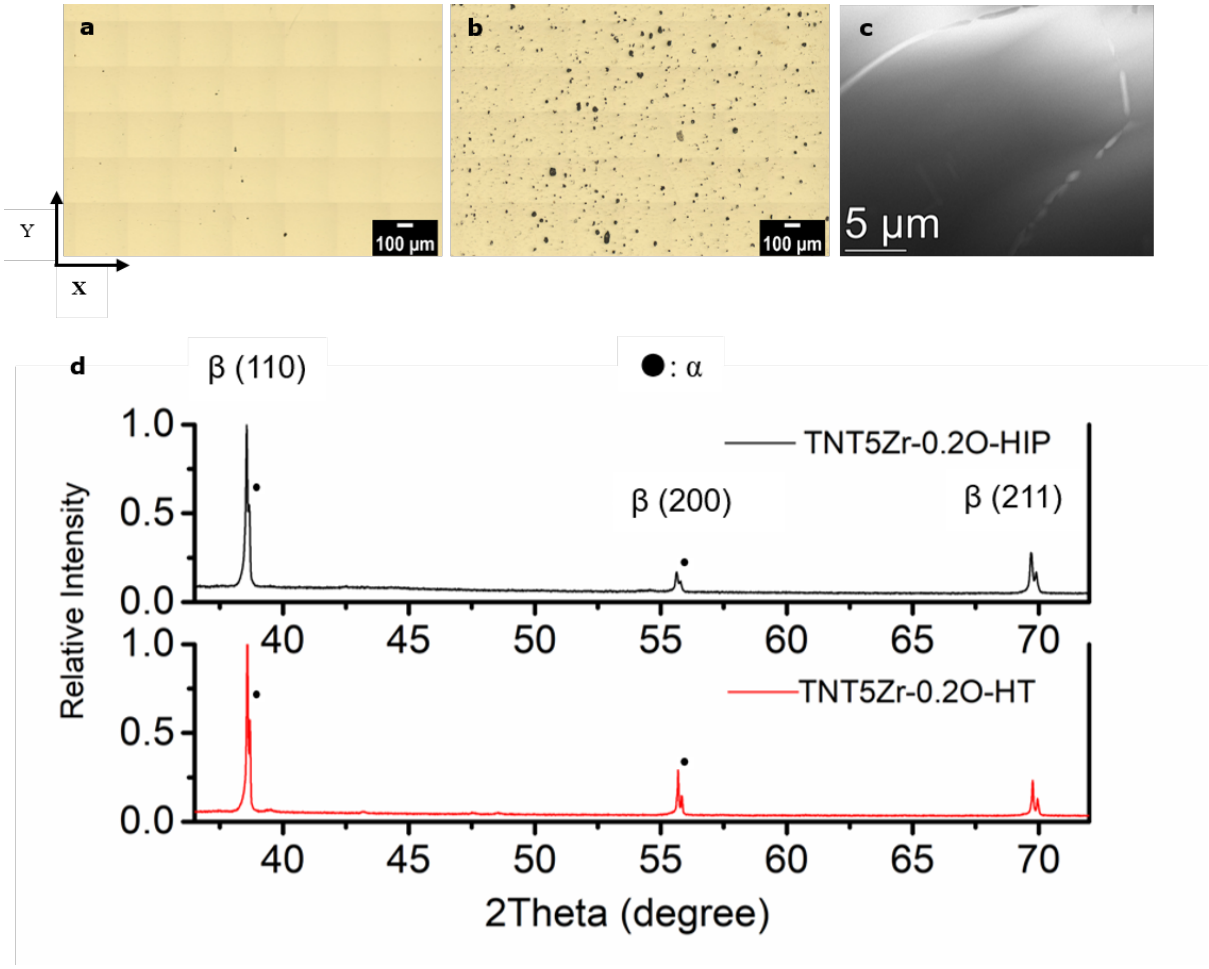

Fig. 1. OM images showing SLMed voids in TNT5Zr-0.2O alloy undergo (a) hot isostatic pressing (HIP) (b) vacuum heat treatment (HT). (c) HAADF image showing grain boundary precipitates in as-HIPed TNT5Zr-0.2O alloy; (d) XRD patterns of the Ti-alloys produced by HIP and HT.

The engineering stress-strain curves of the alloy at two conditions are given in Fig. 2a. It presents the alloys both undergo elastic and plastic deformation till rupture. SEM images (Fig. 2(b-c)) of TNT5Zr-0.2O-HIP alloy fracture reveals the terrace-like grain boundary fracture and intragranular fracture. Similar fracture surface (with voids) is found in TNT5Zr-0.2O-HT alloy (Fig. 2(e-f)), and the high mag. fractographs (Fig. 2(d, g)) show same ductile dimple feature under tension. Besides oxygen solute strengthening mechanism [14] in the two alloys, the nano-sized particles (Fig. 1c) impede grain boundary migration and pin dislocation motion within the grain boundary. Table 1 integrates the as-measured tensile properties of the alloy at two conditions and literature results. TNT5Zr-0.2O-HIP alloy possesses high ultimate tensile strength (UTS) of 1036 ± 26 MPa, and elongation of 3.0% ± 0.3%. By comparison, the TNT5Zr-0.2O-HT alloy shows lower UTS (978 ± 19 MPa) and elastic modulus (49 ± 3

GPa), but higher elongation (4.5% ± 0.6%). The stress concentrations at the edge of keyholes make the voids wall collapse under tension and cracks propagate more easily in that region. Hence, this leads the TNT5Zr-0.2O-HT alloy to yield at a lower confining stress than TNT5Zr-0.2O-HIP; the pore enclosure is not contribute to a better ductility of this alloy.

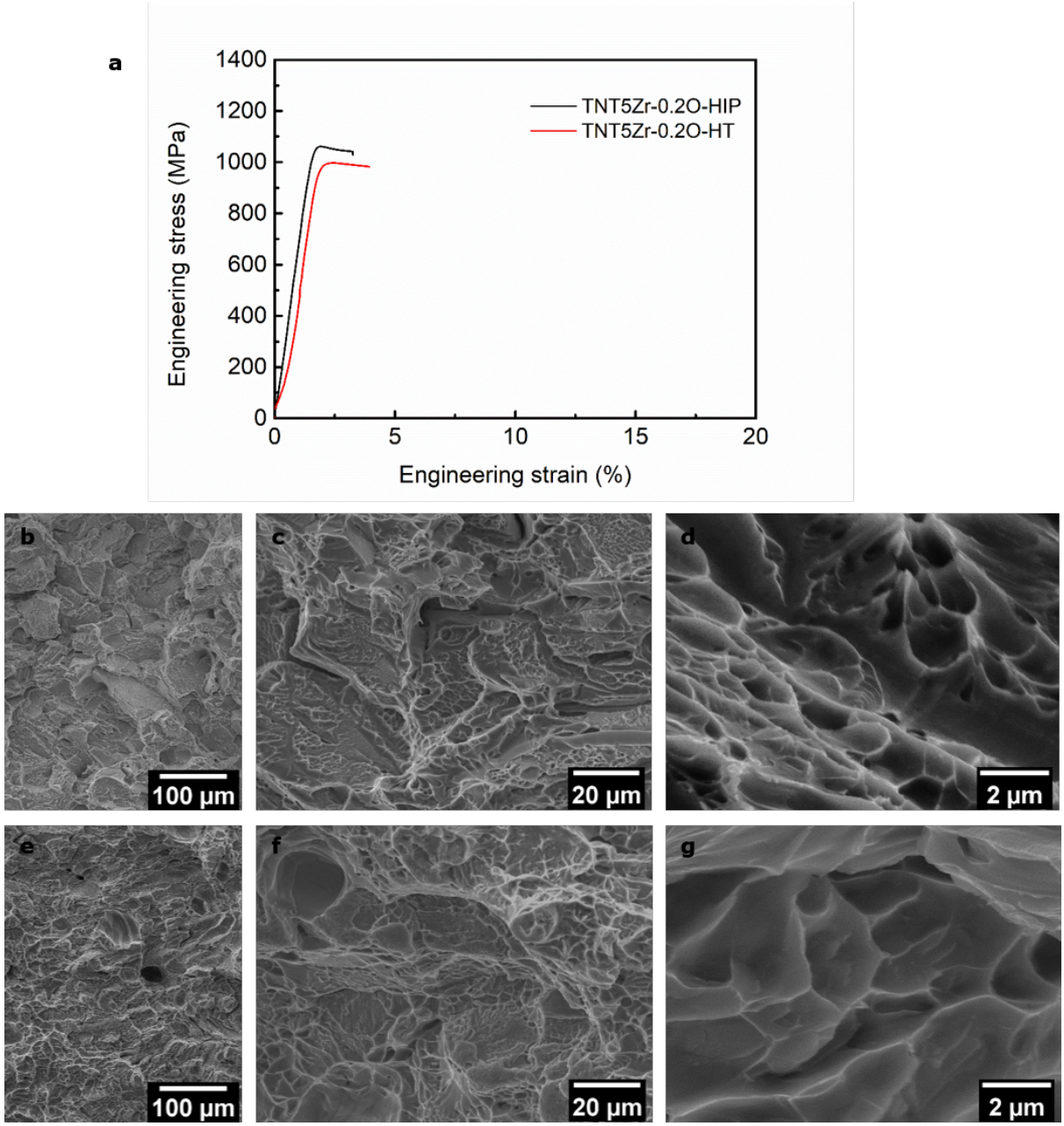

Fig. 2. (a) Engineering stress-strain curves of as-HIPed and as-HTed TNT5Zr-0.2O alloys. (b), (c) and (d) increasing mag. SEM fractographs of TNT5Zr-0.2O-HIP alloy; (e), (f) and (g) increasing mag. SEM fractographs of TNT5Zr-0.2O-HT alloy.

Table 1 Tensile properties of the as-fabricated TNT5Zr-0.2O alloy, and the alloy subjected to different post-processing treatments.

Material	E (GPa)	$\sigma_{0.2}$ (MPa)	σ_{UTS} (MPa)	δ (%)	σ_{UTS}/E
TNT5Zr-0.2O-HIP	69 ± 1	982 ± 6	1036 ± 26	3.0 ± 0.3	14.9 ± 0.7
TNT5Zr-0.2O-HT	49 ± 3	949 ± 16	978 ± 19	4.5 ± 0.6	19.3 ± 1.5
TNT5Zr-0.2O-AF	60 ± 5	938 ± 8	975 ± 12	4.9 ± 0.3	16.3 ± 1.1
TNTZ [15–17]	46-80	447-900	545-950	--	--

4. Conclusions

Ti-34Nb-13Ta-5Zr-0.2O alloy (hereafter termed TNT5Zr-0.2O) with randomly distributed keyhole defects has been fabricated by selective laser melting (SLM). It follows two type of post-processing treatments, namely hot isostatic pressing (HIP) and vacuum heat treatment (HT). XRD analysis shows that the presence of α phase peak in addition to the primary beta phase peaks in both as-HIPed and as-HTed TNT5Zr-0.2O alloys. TEM characterisation confirms the nucleation of discrete nano-sized intergranular precipitates. The mechanical tests demonstrate that TNT5Zr-0.2O-HT alloy possesses lower UTS (978 ± 19 MPa) and elastic modulus (49 ± 3 GPa), but higher elongation (4.5% ± 0.6%) in comparison with TNT5Zr-0.2O-HIP sample. The stress concentrations at the edge of keyholes make the voids wall collapse under tension and cracks propagate more easily in that region. But the pore enclosure fulfilled by HIP is not contribute to a better ductility of this alloy.

5. Acknowledgements

MMA acknowledges the financial support for work provided by Institute of New Materials, Guangdong Academy of Sciences (PI: MMA, grant: 17-0551).

Reference

[1] M. Long, H.J. Rack, Titanium alloys in total joint replacement - A materials science perspective, Biomaterials. (1998). https://doi.org/10.1016/S0142-9612(97)00146-4.

[2] D.M. Gordin, R. Ion, C. Vasilescu, S.I. Drob, A. Cimpean, T. Gloriant, Potentiality of the “gum Metal” titanium-based alloy for biomedical applications, Mater. Sci. Eng. C. (2014). https://doi.org/10.1016/j.msec.2014.08.003.

[3] P. Neacsu, D.M. Gordin, V. Mitran, T. Gloriant, M. Costache, A. Cimpean, In vitro performance assessment of new beta Ti-Mo-Nb alloy compositions, Mater. Sci. Eng. C. (2015). https://doi.org/10.1016/j.msec.2014.11.023.

[4] M. Atapour, A.L. Pilchak, G.S. Frankel, J.C. Williams, Corrosion behavior of β titanium alloys for biomedical applications, Mater. Sci. Eng. C. (2011). https://doi.org/10.1016/j.msec.2011.02.005.

[5] S.H. Huang, P. Liu, A. Mokasdar, L. Hou, Additive manufacturing and its societal impact: A literature review, Int. J. Adv. Manuf. Technol. (2013). https://doi.org/10.1007/s00170-012-4558-5.

[6] J.J. Lewandowski, M. Seifi, Metal Additive Manufacturing: A Review of Mechanical Properties, Annu. Rev. Mater. Res. (2016). https://doi.org/10.1146/annurev-matsci-070115-032024.

[7] A. Matsunawa, J.-D. Kim, N. Seto, M. Mizutani, S. Katayama, Dynamics of keyhole and molten pool in laser welding, J. Laser Appl. (1998). https://doi.org/10.2351/1.521858.

[8] Y.J. Liu, S.J. Li, H.L. Wang, W.T. Hou, Y.L. Hao, R. Yang, T.B. Sercombe, L.C. Zhang, Microstructure, defects and mechanical behavior of beta-type titanium porous structures manufactured by electron beam melting and selective laser melting, Acta Mater. (2016). https://doi.org/10.1016/j.actamat.2016.04.029.

[9] C. Qiu, N.J.E. Adkins, M.M. Attallah, Microstructure and tensile properties of selectively laser-melted and of HIPed laser-melted Ti-6Al-4V, Mater. Sci. Eng. A. (2013). https://doi.org/10.1016/j.msea.2013.04.099.

[10] H. V. Atkinson, S. Davies, Fundamental aspects of hot isostatic pressing: An overview, Metall. Mater. Trans. A Phys. Metall. Mater. Sci. (2000). https://doi.org/10.1007/s11661-000-0078-2.

[11] R. Banerjee, S. Nag, J. Stechschulte, H.L. Fraser, Strengthening mechanisms in Ti-Nb-Zr-Ta and Ti-Mo-Zr-Fe orthopaedic alloys, Biomaterials. (2004). https://doi.org/10.1016/j.biomaterials.2003.10.041.

[12] S. Nag, R. Banerjee, H.L. Fraser, Microstructural evolution and strengthening mechanisms in Ti-Nb-Zr-Ta, Ti-Mo-Zr-Fe and Ti-15Mo biocompatible alloys, in: Mater. Sci. Eng. C, 2005. https://doi.org/10.1016/j.msec.2004.12.013.

[13] ASTM, E1409-13: Standard Test Method for Determination of Oxygen and Nitrogen in Titanium and Titanium Alloys by Inert Gas Fusion, ASTM Stand. (2013).

[14] Q. Yu, L. Qi, T. Tsuru, R. Traylor, D. Rugg, J.W. Morris, M. Asta, D.C. Chrzan, A.M. Minor, Origin of dramatic oxygen solute strengthening effect in titanium, Science (80-.). (2015). https://doi.org/10.1126/science.1260485.

[15] D. Kuroda, M. Niinomi, M. Morinaga, Y. Kato, T. Yashiro, Design and mechanical properties of new β type titanium alloys for implant materials, Mater. Sci. Eng. A. (1998). https://doi.org/10.1016/s0921-5093(97)00808-3.

[16] J. Stráský, P. Harcuba, K. Václavová, K. Horváth, M. Landa, O. Srba, M. Janeček, Increasing strength of a biomedical Ti-Nb-Ta-Zr alloy by alloying with Fe, Si and O, J. Mech. Behav. Biomed. Mater. (2017). https://doi.org/10.1016/j.jmbbm.2017.03.026.

[17] P. Laheurte, F. Prima, A. Eberhardt, T. Gloriant, M. Wary, E. Patoor, Mechanical properties of low modulus β titanium alloys designed from the electronic approach, J. Mech. Behav. Biomed. Mater. (2010). https://doi.org/10.1016/j.jmbbm.2010.07.001.